

Clues to the origin of parsec to kilo-parsec jet misalignments in EGRET sources

Xinwu Cao

¹ Shanghai Astronomical Observatory, Chinese Academy of Sciences, 80 Nandan Road, Shanghai, 200030, China

² National Astronomical Observatories, Chinese Academy of Sciences, China

³ Beijing Astrophysical Center (BAC), Beijing, China

Received ; accepted December 21, 1999

Abstract. The apparent position angle difference ΔPA between parsec and kilo-parsec jets in blazars can be related to the bending properties of the jets. We present correlations between the misalignment ΔPA and the ratio of radio to broad-line emission for a sample of γ -ray blazars. The present study is limited to EGRET sources due to uniform data for the radio and optical properties of these sources being easily available. The broad-line emission is known to be a good indicator of the accretion power for both steep and flat-spectrum quasars. We find significant correlations between ΔPA and the ratio of radio flux (total and radio core flux respectively) to broad-line flux, which is consistent with the beaming scenario. A weak correlation between ΔPA and the ratio of extended radio to broad-line flux might imply that the intrinsic bend of the jet is related with the ratio of jet mechanical power to accretion power.

Key words: galaxies:active– galaxies:jets– quasars:emission lines– accretion, accretion disks

1. Introduction

The recent released third catalog of high-energy γ -ray sources by the EGRET telescope on the Compton Gamma-Ray Observatory contains 66 high-confidence identifications of blazars and 27 lower-confidence potential blazar identifications (Hartman et al. 1999). The γ -ray blazars are relativistically beamed and have strong jet components. The inverse Compton scattering is the most promising process responsible for the γ -ray emission (Marscher & Gear 1985; Bloom & Marscher 1996; Ghisellini & Madau 1996; Böttcher & Dermer 1998). All γ -ray AGNs identified by EGRET are radio-loud with flat spectrum, but not all flat-spectrum AGNs are detectable γ -ray sources. One possibility is that the beaming cone for γ -ray emission is narrower than that for radio emission. In this case, the γ -ray emission could be beamed away from the

line of sight, but the radio emission is still Doppler boosted due to a wider beaming cone (von Montigny et al. 1995).

The apparent position angle difference ΔPA between parsec and kilo-parsec jets can be related to the bending properties of the jets. Many authors have investigated the misalignment angle distributions for the different samples of radio sources (Pearson & Readhead 1988; Conway & Murphy 1993; Appl et al. 1996; Tingay et al. 1998). If the angle between the relativistic jet and the line of the sight is small, the projection effect of beaming can amplify the intrinsic bend of the jet (Conway & Murphy 1993). Several effects such as motion of the host galaxy, collision of the jet with clouds, or precession of the central engine, can thereby cause the bend.

Recently, the concept of jet-disc symbiosis was introduced and the inhomogeneous jet model plus mass and energy conservation in the jet-disc system was applied to study the relation between disc and jet luminosities (Falcke & Biermann 1995; Falcke et al. 1995; Falcke & Biermann 1999). An effective approach to study the link between these two phenomena is to explore the relationship between luminosity in line emission and kinetic power of jets in different scales (Rawlings & Saunders 1991; Celotti, Padovani & Ghisellini 1997). Rawlings & Saunders (1991) derived the total jet kinetic power Q_{jet} and found a correlation between Q_{jet} and the narrow line luminosity L_{NLR} . Similar correlations between line and radio emission have also been found by some authors (Cao & Jiang 1999; Xu et al. 1999; Willott et al. 1999). The optical line region is photoionized by a nuclear source (probably radiation from the disk), so the optical line emission is a better accretion power indicator than the optical continuum radiation may be enhanced by relativistically beamed synchrotron radiation for some flat-spectrum quasars (Celotti et al. 1997). The extended radio emission which is not affected by beaming may reflect the jet power Q_{jet} . Thus, the ratio of extended radio to broad-line flux reflects the ratio of jet power to accretion power. In this work, we present correlations between the misalignment ΔPA and the ratio of radio to broad-line emission for a sample of γ -ray blazars. In Sect. 2, we describe the sample of sources. The

results are contained in Sect. 3. The last section includes the discussion.

2. The sample

Complete information on the line spectra is available for very few sources in our sample, since different lines are observed for the sources at different redshifts. We have to estimate the total broad-line flux from the available observational data. There is not a solidly established procedure to derive the total broad-line flux and we therefore adopt the method proposed by Celotti et al. (1997). The following lines: Ly α , C IV, Mg II, H γ , H β and H α , which contribute the major parts in the total broad-line emissions, are used in our estimate. We use the line ratios reported by Francis et al. (1991) and add the contribution from line H α to derive the total broad-line flux (see Celotti et al. 1997 for details). We then search the literature to collect data on broad-line fluxes. We only consider values of line fluxes (or luminosities) given directly or the equivalent width and the continuum flux density at the corresponding line frequency which are reported together in the literature. When more than one value of the same line flux was found in the literature, we take the most recent reference.

We start with the γ -ray blazars identified by Hartman et al. (1999) including lower-confidence blazars. There are 79 AGNs with available redshifts in the third EGRET catalog. Among these sources, we search the literature extensively and find 44 sources with sufficient line data to estimate the total broad-line flux. The remainder of the sources that lack broad-line flux data include 9 BL Lac objects and 26 quasars. The broad-line fluxes have not been measured due to weak line emission for the BL Lac objects. The situation for the quasars is quite different from the BL Lac objects. We note that the spectroscopic observations for most of these 26 quasars have been performed. However, the line data of these quasars are usually incomplete, i.e., only the equivalent width, line profile or line-to-continuum ratio is given, but the continuum flux density at the given frequency is not available probably due to the specific purpose of the literature or the problem of calibration. Only a bit more than half of the γ -ray sources with known redshifts have sufficient data, such that the total broad-line flux can be estimated. This is similar to the situation in Cao & Jiang (1999). In their work, 198 sources within the starting sample of 378 sources have suitable data to derive the total broad-line flux. No evidence shows that the lack of broad-line flux for these sources would affect the main results of present analyses, though it leads to a highly incomplete sample for present study. The further spectroscopic observations on these sources would be helpful. We collect the data of all sources with both the broad-line flux and the misalignment angle Δ PA between parsec and kilo-parsec jets, which leads to a sample of 34 blazars (we add the TeV γ -ray objects: Mkn501 to

the sample, which is not listed in the EGRET catalog). There are 26 quasars and 8 BL Lac objects in this sample, in which 7 sources are lower-confidence potential blazar identifications and two TeV γ -ray objects: Mkn421 and Mkn501. The broad-line data are listed in Table 1. We compile the data of the extended radio flux density at 5 GHz in the rest frame of the source in column (9) of Table 1. The data given at the wavelength other than 5 GHz are K-corrected to 5 GHz in the rest frame of the source assuming $\alpha_{\text{ext}} = -0.75$ ($f_{\text{ext}} \propto \nu^{\alpha_{\text{ext}}}$).

We also give the core flux density data at two different frequencies for each source in the sample, and a two-point spectral index is then derived for the core of the source. The core flux density at 5 GHz in the rest frame of the source is available by K-correction. The misalignment between kilo-parsec and parsec jets Δ PA are taken from the literature. For a few sources, different values of Δ PA are given by different authors usually due to the complex jet structures. We take the minimum Δ PA for these sources. All data of the core flux density and the misalignment angle Δ PA are given in table 2.

The misalignment angle Δ PA is given by the comparison between the VLA and VLBI maps. We note that only one position angle (VLA or VLBI) is available for some sources. Only the VLA position angle is available for the sources 0414–189 and 0954+556. There are five sources: 0454–234, 1504–166, 1741–038, 2200+420 and 2320–035, of which only the VLBI position angle is available. One reason is that these sources are too compact. High dynamic range VLA maps of many sources sufficient to reveal weak kilo-parsec structure are not available. Therefore, further radio observations on these sources might reveal their misalignment information. Further spectroscopic observations are also necessary to complete the sample.

3. Results

The distribution of Δ PA of the sample is plotted in Fig. 1 and appears bimodal, which is similar to that given by Pearson & Readhead (1988). Such distribution can be explained by projection of the helical jet (Conway & Murphy 1993). In Fig. 2 we plot the relation between the apparent misalignment Δ PA and the ratio of the total radio flux at 5 GHz to the broad-line flux. The radio flux density is K-corrected to the rest frame of the source. A correlation is found at 99.9 per cent significant level for the whole sample using Spearman's correlation coefficient ρ . A slightly less significant correlation is present for quasars in the sample. We also find a significant correlation between Δ PA and the ratio of the VLBI core flux to the broad-line flux at the level 99.99 per cent, where the VLBI core flux density is also K-corrected to the rest frame of the source at 5 GHz (see Fig. 3). In Fig. 4 we plot the relation between the apparent misalignment Δ PA and the ratio of the extended radio flux at 5 GHz in the rest frame of

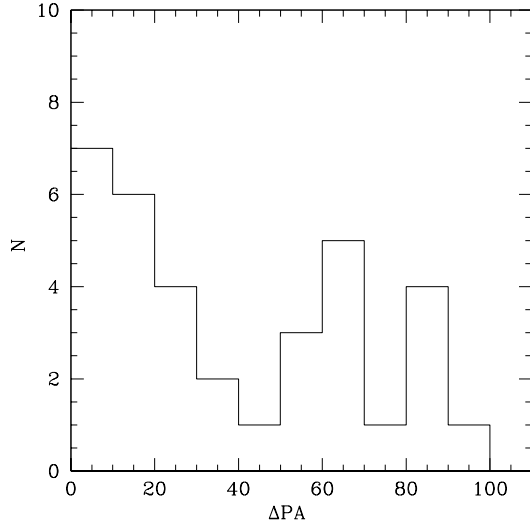


Fig. 1. The ΔPA distribution of the sample.

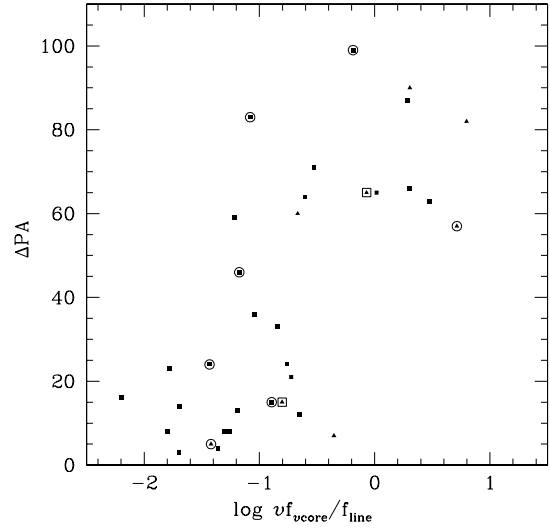


Fig. 3. The relation between the misalignment ΔPA and the ratio of VLBI core flux to the broad-line flux (symbols as in Fig. 2.).

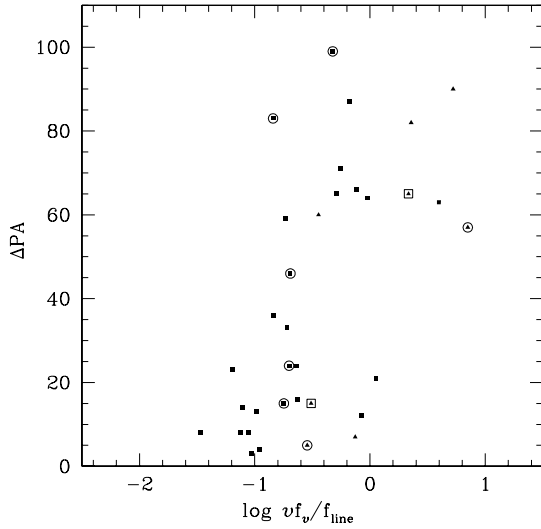


Fig. 2. The relation between the misalignment ΔPA and the ratio of radio to the broad-line flux. The full squares represent the quasars, and the full triangles represent the BL Lac objects, while large circles denote the lower-confidence blazar identifications by EGRET and large squares denote the TeV γ -ray objects.

the source to the broad-line flux. A weak correlation at 90 per cent significance shows that a trend for sources with higher ratios have larger misalignment ΔPA .

In present sample, there are two TeV γ -ray sources: Mkn421 (1101+384) and Mkn501 (1652+398). We know that the three TeV γ -ray objects are quite different from other γ -ray sources (Coppi & Aharonian 1999a,b). Only

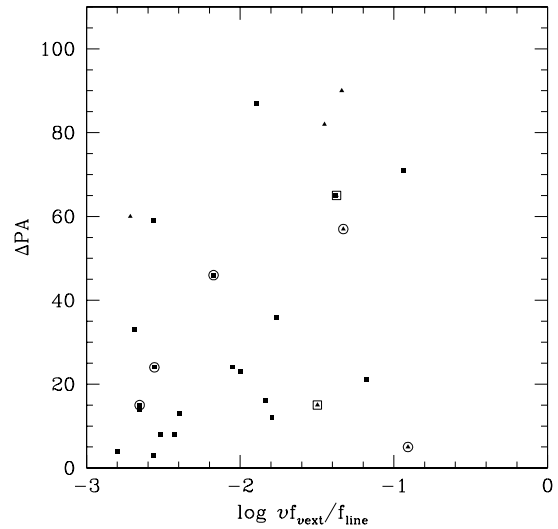


Fig. 4. The relation between the misalignment ΔPA and the ratio of the extended radio flux to the broad-line flux (symbols as in Fig. 2.).

Mkn421 is listed in the third EGRET catalog (Hartman et al. 1999). However, we cannot find obvious different behaviours for these two TeV γ -ray objects from the remains in the sample (see Figs. 2 – 4, labeled by large squares).

The redshifts of the sources in our sample ranges from 0.031 to 2.286, which means that the spatial resolution of VLA and VLBI are very different. However, the angular resolution is about same for these sources, which would

probably affect the correlation analyses (Appl et al. 1996). We therefore group the sources into low ($z < 0.5$) and high ($z > 0.5$) redshift objects. For the latter, the angular to linear scale mapping is approximately constant. We re-analyze the correlations and find a correlation between ΔPA and the ratio of the radio core flux to the broad-line flux at 99.94 per cent significant level for the 24 objects with $z > 0.5$.

4. Discussion

Recently, Serjeant et al. (1998) found a correlation between radio and optical continuum emission for a sample of steep-spectrum radio quasars that is evidence for a link between accretion process and jet power. Their sample is limited to the steep-spectrum quasars to reduce the Doppler beaming effect in the optical waveband. A similar correlation is given by Carballo et al (1999) for the B3-VLA sample. Cao & Jiang (1999) present a correlation between radio and broad-line emission for a sample of radio quasars including both flat-spectrum and steep-spectrum quasars. They adopted the broad-line emission instead of the optical continuum in their investigation to avoid the beaming effect on optical emission. The jet power Q_{jet} is proportional to the bulk Lorentz factor of the jet, and also depends on the size of the jet and the particle density in the jet (Celotti & Fabian 1993). The apparent misalignment may be affected by the angle between the direction of VLBI jet and the sight line if the angle is small (Conway & Murphy 1993). The total radio flux density and VLBI core flux density are both strongly increased by beaming in core-dominated radio blazars. The sources with higher ratio may therefore have higher Doppler factors. So, the correlations between ΔPA and $\nu f_{rad}/f_{line}$ or $\nu f_{core}/f_{line}$ can be explained by the beaming effects. Impey et al. (1991) found that the sources with higher fractional optical polarization tend to have relatively larger misalignment ΔPA between VLBI and parsec structures, which is consistent with both large apparent misalignments and optical fractional polarization being correlated with large beaming and small angles to the line of sight.

The extended radio emission may also be correlated to the jet power Q_{jet} (see Fig. 4). If this is true, the ratio of the extended radio flux to the broad-line flux may reflect the ratio of the jet power to the disk luminosity: Q_{jet}/L_{acc} . The weak correlation between ΔPA and the ratio of extended radio to broad-line flux might imply that the intrinsic bend of the jet is related with the ratio of jet mechanical power to accretion power.

Jets in quasars may be powered by rotating black holes in the nuclei (Blandford & Znajek 1977; Moderski et al. 1998). The jet power Q_{jet} is then related to the rotational energy of the black hole according to the BZ mechanism. Hence, the ratio of radio to broad-line flux might be related to the angular momentum of the black hole to some extent. Also, we know that the variation of the rotation

axis of the black hole caused by the Lense-Thirring effect can result in a change of the orientation of the nuclei jet (Bardeen & Petterson 1975; Scheuer & Feiler 1996), which may lead to the different ejected orientations between small and large scale jets. The faster rotating black hole may cause the jet ejected orientation changing more rapidly, which leads to a larger intrinsic bend of the jet.

More recently, Ghosh & Abramowicz (1997), Livio et al. (1999) have shown that the electromagnetic output from the inner disc is generally expected to dominate over that from the hole. If this is the case for the γ -ray AGNs, the jet power Q_{jet} from the disc is mainly determined by the poloidal magnetic field B_{pd} at the disc surface. A tentative explanation on the relation in Fig. 4. is that both bending and the jet power could be increased by having large magnetic fields in the accretion disk.

The further study on this problem for a larger sample of core-dominated radio quasars will be in our future work, and we can then check whether the correlations are properties only of EGRET sources or of all blazars in general.

Acknowledgements. I thank the referee for his helpful comments and suggestions that improved the presentation of this paper, X.Y. Hong is thanked for helpful discussion on the measurement of misalignment angle. The support by NSFC and Pandeng Plan is gratefully acknowledged. This research has made use of the NASA/IPAC Extragalactic Database (NED), which is operated by the Jet Propulsion Laboratory, California Institute of Technology, under contract with the National Aeronautic and Space Administration.

References

- Antonucci R.R.J., Ulvestad J.S., 1985, ApJ 294 158 (AU85)
- Appl S., Sol H., Vicente L., 1996, A&A 310, 419 (A96)
- Baldwin J.A., Wampler E.J., Gaskell C.M., 1989, ApJ 338, 630(B89)
- Bardeen J.M., Petterson J.A., 1975, ApJ 195, L65
- Bergeron J., Kunth D., 1984, MNRAS 207, 263(BK84)
- Blandford R.D., Znajek R.L., 1977, MNRAS 179, 433
- Bloom S.D., Marscher A.P., 1996, ApJ 461, 657
- Böttcher M., Dermer C.D., 1998, ApJ 501, L51
- Browne I.W.A., 1987, Superluminal radio sources, J.A. Zensus & T.J. Pearson, eds., Cambridge Univ. Press, p. 129 (B87)
- Browne I.W.A., Clark R.R., Moore P.K. et al., 1982, Nat 299, 788 (B82)
- Browne I.W.A., Murphy D.W., 1987, MNRAS 226, 601 (BM87)
- Browne I.W.A., Perley R.A., 1986, MNRAS 222, 149 (BP86)
- Cao X., Jiang D.R., 1999, MNRAS 307, 802
- Carballo R., Gonzalez-Serrano J.I., Benn C.R., Sanchez S.F., Vigotti M., 1999, MNRAS 306, 137
- Celotti A., Fabian A.C., 1993, MNRAS 264, 228
- Celotti A., Padovani P., Ghisellini G., 1997, MNRAS 286, 416
- Conway J.E., Murphy D.W., 1993, ApJ 411, 89 (CM93)
- Coppi P.S., Aharonian F.A., 1999a, ApJ 521, L33
- Coppi P.S., Aharonian F.A., 1999b, astro-ph. 9903160
- di Serego Alighieri S., Danziger I.J., Morganti R. et al., 1994, MNRAS 269, 998(d94)

- Falcke H., Biermann P.L., 1995, *A&A* 293, 665
- Falcke H., Biermann P.L., 1999, *A&A* 342, 49
- Falcke H., Malkan M.A., Biermann P.L., 1995, *A&A* 298, 375
- Fey A.L., Charlot P., 1997, *ApJS* 111, 95 (FC97)
- Fey A.L., Clegg A.W., Fomalont E.B., 1996, *ApJS* 105, 299 (F96)
- Francis P.J., Hewett P.C., Foltz C.B. et al., 1991, *ApJ* 373, 465
- Gabuzda D.C., Cawthorne T.V., Roberts D.H. et al., 1992, *ApJ* 388, 40 (G92)
- Ghisellini G., Madau P., 1996, *MNRAS* 280, 67
- Ghosh P., Abramowicz M.A., 1997, *MNRAS* 292, 887
- Hartman R.C., Bertsch D.L., Bloom S.D. et al., 1999, *ApJS* 123, 79
- Hintzen P., Ulvestad J., Owen F., 1983, *AJ* 88, 709 (H83)
- Hong X.Y., Jiang D.R., Shen Z.Q., 1998, *A&A* 330, L45 (H98)
- Hooimeyer J.R.A., Barthel P.D., Schilizzi R.T. et al., 1992, *A&A* 261, 18 (Ho92a)
- Hooimeyer J.R.A., Schilizzi R.T., Miley G.K. et al., 1992, *A&A* 261, 25 (Ho92b)
- Hummel C.A., Muxlow T.W.B., Krichbaum T.P. et al., 1992, *A&A* 266, 93 (H92)
- Impey C.D., Lawrence C.R., Tapia S., 1991, *ApJ* 375, 46
- Jackson N., Browne J.W.A., 1991, *MNRAS* 250, 414 (JB91)
- Junkkarinen V., 1984, *PASP* 96, 539 (J84)
- Keel W.C., 1986, *ApJ* 302, 296 (K86)
- Kellermann K.I., Vermeulen R.C., Zensus J.A. et al., 1998, *AJ* 115, 1295 (K98)
- Kollgaard R.L., Wandle J.F.C., Roberts D.H. et al., 1992, *AJ* 104, 1687 (K92)
- Lawrence C.R., Zucker J.R., Readhead A.C.S. et al., 1996, *ApJS* 107, 541 (L96)
- Linfield R.P., Levy G.S., Edwards C.D. et al., 1990, *ApJ* 358, 350 (L90)
- Livio M., Ogilvie G.I., Pringle J.E., 1999, *ApJ* 512, 100
- Madau P., Ghisellini G., Persic M., 1987, *MNRAS* 224, 257 (M87)
- Marscher A.P., Gear W.K., 1985, *ApJ* 298, 114
- Marziani P., Sulentic J.W., Dultzin-Hacyan D. et al., 1996, *ApJS* 104, 37 (Ma96)
- Moderski R., Sikora M., Lasota J.P., 1998, *MNRAS* 301, 142
- Moellenbrock G.A., Fujisawa K., Preston R.A. et al., 1996, *AJ* 111, 2174 (Mo96)
- Morabito D.D., Niell A.E., Preston R.A. et al., 1986 *AJ* 91, 1038 (M86)
- Morganti R., Ulrich M.H., Tadhunter C.N. et al., 1992, *MNRAS* 254, 546 (M92)
- Murphy D.W., Browne I.W.A., Perley R.A., 1993, *MNRAS* 264, 298 (M93)
- Mutel R.L., 1990, in *Parsec-scale radio jets*, J.A. Zensus, T.J. Pearson, eds., Cambridge Univ. Press, p. 98 (M90)
- Neugebauer G., Oke J.B., Beckline E.E. et al., 1979, *ApJ* 230, 79 (N79)
- Osmer P.S., Porter A.C., Green R.F., 1994, *ApJ* 436, 678 (O94)
- Pauliny-Toth I.I.K., Porcas R.W., Zensus J.A. et al., in *IAU symposium 110: VLBI and compact radio sources*, R. Fanti, K.I. Kellermann, S. Setti, eds., Dordrecht: Reidel, p. 149 (P84)
- Pearson T.J., Readhead A.C.S., 1988, *ApJ* 328, 114 (PR88)
- Perley R.A., 1982, *AJ* 87, 859 (P82)
- Polatidis A.G., Wilkinson P.N., Xu W. et al., 1995, *ApJS* 98, 1 (P95)
- Preston R.A., Morabito D.D., Williams J.G. et al., 1985, *AJ* 90, 1599 (P85)
- Rawlings S.G., Saunders R.D.E., 1991, *Nat* 349, 138
- Richstone D.O., Schmidt M., 1980, *ApJ* 235, 361 (RS80)
- Roberts D.H., Gabuzda D.C., Wardle J.F.C., 1987, *ApJ* 323, 536 (R87)
- Rumney J., Padrielli L., Barthel N. et al., 1984, *A&A* 135, 289 (R84)
- Rudy R.J., 1984, *ApJ* 284, 33 (R84)
- Rusk R.E., 1988, Ph. D. thesis, Univ. Toronto (R88)
- Scarpa R., Falomo R., Pian E. et al., 1995, *A&A* 303, 730 (S95)
- Scheuer P.A.G., Feiler R., 1996, *MNRAS* 282, 291
- Serjeant S., Rawlings S., Maddox S.J. et al., 1998, *MNRAS* 294, 494
- Shen Z.Q., Wan T.S., Moran J.M. et al., 1997, *AJ* 114, 1999 (S97)
- Shen Z.Q., Wan T.S., Moran J.M. et al., 1998, *AJ* 115, 1357 (S98)
- Stickel M., Fried W., Kühr H., 1989, *A&AS* 80, 103 (S89)
- Stickel M., Fried W., Kühr H., 1993a, *A&AS* 98, 393 (S93a)
- Stickel M., Kühr H., 1993, *A&AS* 101, 521 (SK93)
- Stickel M., Kühr H., Fried W., 1993b, *A&AS* 97, 483 (S93b)
- Stockton A., MacKenty J.W., 1987, *ApJ* 316, 584 (SM87)
- Tadhunter C.N., Morganti R., Alighieri S. et al., 1993, *MNRAS* 263, 999 (T93)
- Tingay S.J., Edwards P.G., Costa M.E. et al., 1996, *ApJ* 464, 170 (T96)
- Tingay S.J., Murphy D.W., Edwards P.G., 1998, *ApJ* 500, 673 (T98)
- Unwin S.C., 1987, *Superluminal radio sources*, J.A. Zensus & T.J. Pearson, eds., Cambridge Univ. Press, p. 34 (U87)
- von Montigny C., Bertsch D.L., Chiang J. et al., 1995, *A&A* 299, 680
- Wampler E.J., Gaskell C.M., Burke W.L., 1984, *ApJ* 276, 403 (W84)
- Wardle J.F.C., Roberts D.H., Brown L.F. et al., 1990, in *Parsec-scale radio jets*, J.A. Zensus, T.J. Pearson, eds., Cambridge Univ. Press, p. 98 (W90)
- Wehrle A.E., Cohen M.H., Unwin S.C. et al., 1992, *ApJ* 391, 589 (W92)
- Wills B.J., Pollock J.T., Aller H.D. et al., 1983, *ApJ* 274, 62 (W83)
- Wills B.J., Thompson K.L., Han M. et al., 1995, *ApJ* 447, 139 (W95)
- Xu C., Livio M., Baum S., 1999, *AJ* 118, 1169
- Xu W., Readhead A.C.S., Pearson T.J. et al., 1995, *ApJS* 99, 297 (X95)
- Zhang F.J., Baath L.B., 1990, *A&A* 236, 47 (ZB90)

Table 1. Data of radio and broad-line fluxes.

Source (1)	Class. (2)	z (3)	$\log f_{BLR}$ (4)	Lines (5)	Refs. (6)	f_{5G} (Jy) (7)	α_{11-6} (8)	f_{ext} (mJy) (9)	Refs. (10)
0119+041 [†]	Q	0.637	-12.61	Mg II, H γ , H β	JB91,RS80	1.67	0.04	32.9	BM87
0234+285 [†]	Q	1.210	-12.66	C IV	W84	1.44	-0.24	9.75	BM87
0235+164	BL	0.940	-13.79	Mg II	S93a	2.85	1.03	11.5	M93
0336-019	Q	0.852	-12.55	Mg II, H γ , H β	B89,JB91	2.86	0.30	49.7	BM87
0420-014	Q	0.915	-12.70	Mg II	B89	1.46	0.01	8.23	BM87
0440-003	Q	0.844	-13.00	Mg II, H γ , H β	B89,JB91	2.61	-0.29	32.15	BM87
0458-020	Q	2.286	-13.28	Ly α , C IV	B89	1.74	-0.08	121.8	BM87
0521-365 [†]	BL	0.055	-11.80	Ly α , H β , H α	S95	9.29	-0.43	3900	AU85
0537-441	BL	0.896	-12.55	Mg II	S93a	4.00	0.06	10.95	BM87
0539-057 [†]	Q	0.839	-13.42	Mg II	SK93	1.55	1.41	...	
0804+499 [†]	Q	1.433	-12.71	C IV, Mg II	L96	2.05	0.47	1.84	M93
0836+710	Q	2.172	-12.12	Ly α , C IV, Mg II	L96	2.59	-0.32	33.5	M93
0851+202	BL	0.306	-12.88	Mg II, H β , H α	S89,S93a	2.62	0.11	1.87	K92
0954+658	BL	0.367	-14.04	H α	L96	1.46	0.35	8.32	K92
1101+384	BL	0.031	-12.94	H α	M92	0.73	-0.09	72.8	AU85
1127-145 [†]	Q	1.187	-12.13	Ly α	W95	6.57	0.03	40.9	BM87
1156+295	Q	0.729	-12.49	Mg II	W83	1.54	-0.1	111.4	AU85
1222+216	Q	0.435	-12.11	H β	SM87	1.26	-0.40	156.9	H83
1226+023	Q	0.158	-10.27	Ly α , C IV, H β , H α	O94,JB91,Ma96	42.85	0.15	4003	BM87
1253-055	Q	0.536	-12.42	Ly α , C IV, Mg II, H β , H α	W95,Ma96,N79	14.95	0.30	502.5	BM87
1334-127	Q	0.539	-12.88	Mg II	S93b	2.24	0.17	109.9	BP86
1424-418	Q	1.522	-13.20	Mg II	S89	3.13	0.28	...	
1510-089	Q	0.361	-12.00	Ly α , Mg II, H γ , H β , H α	N79,T93,O94,BK84	3.08	0.31	80.6	BM87
1514-241 [†]	BL	0.042	-13.86	H β	T93	2.00	-0.16	12.8	AU85
1611+343	Q	1.401	-12.17	Ly α , C IV	W95	2.67	0.10	40.9	BM87
1622-253	Q	0.786	-13.80	Mg II, H β	d94	2.08	-0.14	...	
1633+382	Q	1.814	-12.52	Ly α , C IV, Mg II	L96	4.02	0.73	9.7	BM87
1652+398	BL	0.0337	-13.50	H α	L96	1.42	0.06	26.9	AU85
1725-044	Q	0.296	-12.35	H β	R84	1.24	0.76	5.1	BM87
1730-130	Q	0.902	-12.78	H γ , H β	J84	6.99	0.8	42.8	BM87
1739+522	Q	1.379	-12.90	C IV, Mg II	L96	1.98	0.68	6.8	BM87
2230+114	Q	1.037	-11.87	Ly α , C IV	W95	3.61	-0.50	74.4	BM87
2251+158	Q	0.859	-11.88	Ly α , C IV, Mg II, H γ , H β	N79,W95,JB91	17.42	0.64	386.7	BM87
2351+456	Q	1.992	-13.58	C IV, Mg II	L96	1.42	-0.05	...	

Notes for the table 1. Q: quasars; BL: BL Lac objects. †: lower-confidence blazar identification.

Column (1): IAU source name. Column (2): classification of the source. Column (3): redshift. Column (4): estimated total broad-line flux ($\text{erg s}^{-1} \text{cm}^{-2}$). Column (5): lines from which the total f_{line} has been estimated. Column (6): references for the line fluxes. Column (7): radio flux density (in Jy) at 5 GHz. Column (8): two-point spectral index between 6–11 cm. Column (9): extended radio flux density (in mJy) at 5GHz in the rest frame of the source. Column (10): references for the extended radio flux density.

References:

AU85: Antonucci & Ulvestad (1985), B89: Baldwin et al. (1989), BK84: Bergeron & Kunth (1984), BM87: Browne & Murphy (1987), BP86: Browne & Perley (1986), d94: di Serego Alighieri et al. (1994), H83: Hintzen et al. (1983), J84: Junkkarinen et al. (1984), JB91: Jackson & Browne (1991), K92: Kollgaard et al. (1992), L96: Lawrence et al. (1996), M92: Morganti et al. (1992), M93: Murphy et al. (1993), Ma96: Marziani et al. (1996), N79: Neugebauer et al. (1979), O94: Osmer et al. (1994), R84: Rudy (1984), RS80: Richstone & Schmidt (1980), S89: Stickel et al. (1989), S93a: Stickel et al. (1993a), S93b: Stickel et al. (1993b), S95: Scarpa et al. (1995), SK93: Stickel & Kühr (1993), SM87: Stockton & MacKenty (1987), T93: Tadhunter et al. (1993), W83: Wills et al. (1983), W84: Wampler et al. (1984), W95: Wills et al. (1995).

Table 2. Data of radio core flux density and Δ PA.

Source (1)	ν_1 (2)	f_1 (3)	ν_2 (4)	f_2 (5)	Refs. (6)	PA_{kpc} (7)	PA_{pc} (8)	Refs. (9)	Δ PA (10)	ref. (11)
0119+041 [†]	2.29	1.0	8.4	0.53	P85,M86	146	100	P82,K98	46	
0234+285 [†]	2.32	1.78	8.55	1.32	F96	-25	-10	M93,F96	15	H98
0235+164	5	4.45	22	3.44	S97,Mo96	-37	45	M93,M90	82	H98
0336-019	2.29	1.4	22	2.08	P85,Mo96	-15	9	P82,W92	24	A96
0420-014	2.32	3.1	8.55	1.19	F96	180	-147	AU85,F96	33	H98
0440-003	2.32	2.11	8.55	0.85	FC97	90	102	P82,FC97	12	H98
0458-020	5	2.62	22	0.82	S97,Mo96	-126	-55	B87,W92	71	A96
0521-365 [†]	4.8	1.2	8.4	1.65	T98	305	310	K86,T96	5	H98
0537-441	4.851	4.0	8.4	2.55	T96,M86	305	5	P82,T96	60	H98
0539-057 [†]	2.32	0.77	8.55	0.89	FC97	50	149	P82, FC97	99	
0804+499 [†]	5	1.344	22	0.54	PR88,Mo96	199	116	CM93	83	CM93
0836+710	1.7	1.11	5	1.045	H92,PR88	200	214	P82,PR88	14	H98
0851+202	2.32	1.23	8.55	1.6	FC97	253	246	R87	7	K92
0954+658	2.29	0.43	5	0.48	P85,G92	206	-65	P82,M90	90	CM93
1101+384	1.7	0.224	5	0.366	P95,X95	301	316	ZB90,T98	15	T98
1127-145 [†]	5	1.91	8.387	1.4	S97,T98	41	65	R88,W92	24	H98
1156+295	2.32	0.94	8.55	1.00	F96	60	24	M90,T98	36	T98
1222+216	2.29	0.33	5	0.36	P85,Ho92b	23	Ho92a
1226+023	5	21.8	22	7.79	S98,Mo96	222	-130	P82,W90	8	H98
1253-055	2.3	3.97	8.4	2.12	M87,L90	202	-137	P82,U87	21	M90
1334-127	2.32	3.45	8.55	4.27	F96	90	155	P82,F96	65	
1424-418	2.29	0.37	5	1.36	P85,S98	56	-10	T98	66	T98
1510-089	2.32	2.97	8.55	1.56	FC97	160	173	P82,R84	13	H98
1514-241 [†]	5	1.53	22	0.41	S98,Mo96	120	177	P82,S98	57	
1611+343	2.32	4.16	8.55	2.14	FC97	-170	-178	M93,F96	8	H98
1622-253	2.32	1.67	8.55	1.7	FC97	303	6	P82,F96	63	H98
1633+382	2.32	2.41	8.55	1.03	FC97	-60	-64	X95,PR88	4	H98
1652+398	2.32	0.69	8.55	0.49	FC97	45	110	P95,X95	65	T98
1725-044	2.32	0.84	8.55	0.51	FC97	105	113	P82,FC97	8	
1730-130	5	2.34	8.387	8.8	S97,T98	0	273	T98	87	T98
1739+522	2.32	0.94	8.55	0.44	FC97	260	319	P82,PR88	59	A96
2230+114	2.32	2.11	8.55	1.2	FC97	140	137	P82,B87	3	M90
2251+158	2.29	3.4	5	0.9	P85,M87	-49	-65	B82,P84	16	B87
2351+456	5	0.323	22	0.42	PR88,Mo96	25	321	T98	64	T98

Notes for the table 2. †: lower-confidence blazar identification.

Column (1): IAU source name. Column (2)-(4): VLBI observation frequencies (in GHz) and core flux density (in Jansky). Column (6): references for core flux density. Column (7) and (8): position angles (degree) for kilo-parsec and parsec jet components. Column (9): references for position angles. Column (10) and (11): difference of position angle (degree) between kilo-parsec and parsec jet components and the reference in which the Δ PA is given.

References:

A96: Appl et al. (1996), AU85: Antonucci & Ulvestad (1985), B82: Browne et al. (1982), B87: Browne (1987), CM93: Conway & Murphy (1993), F96: Fey et al. (1996), FC97: Fey & Charlot (1997), G92: Gabuzda et al (1992), H92: Hummel et al. (1992), Ho92a: Hooimeyer et al. (1992a), Ho92b: Hooimeyer et al. (1992b), H98: Hong et al. (1998), K86: Keel (1986), K92: Kollgaard et al. (1992), K98: Kellermann et al. (1998), L90: Linfield et al. (1990), M86: Morabito et al. (1986), M87: Madau et al. (1987), M90: Mutel (1990), M93: Murphy et al. (1993), Mo96: Moellenbrock et al. (1996), P82: Perley (1982), P84: Pauliny-Toth et al. (1984), P85: Preston et al. (1985), P95: Polatidis et al. (1995), PR88: Pearson & Readhead (1988), R84: Romney et al. (1984), R87: Roberts et al. (1987), R88: Rusk (1988), S97: Shen et al. (1997), S98: Shen et al. (1998), T96: Tingay et al. (1996), T98: Tingay et al. (1998), U87: Unwin (1987), W90: Wardle et al. (1990), W92: Wehrle et al. (1992), X95: Xu et al. (1995). ZB90: Zhang & Baath (1990).